Model for computing kinetics of the graphene edge epitaxial growth on copper

Mikhail Khenner
Department of Mathematics, Western Kentucky University, Bowling Green, Kentucky 42101, USA
and Applied Physics Institute, Western Kentucky University, Bowling Green, Kentucky 42101, USA
(Received 24 January 2016; revised manuscript received 4 April 2016; published 29 June 2016)

A basic kinetic model that incorporates a coupled dynamics of the carbon atoms and dimers on a copper surface is used to compute growth of a single-layer graphene island. The speed of the island's edge advancement on Cu[111] and Cu[100] surfaces is computed as a function of the growth temperature and pressure. Spatially resolved concentration profiles of the atoms and dimers are determined, and the contributions provided by these species to the growth speed are discussed. Island growth under the conditions of a thermal cycling is studied.

DOI: 10.1103/PhysRevE.93.062806

I. INTRODUCTION

Epitaxial growth of high-quality, large-area single- and multilayer graphene sheets on a transition-metal substrate is presently a focus of research efforts worldwide, as has been discussed in several review articles [1–3]. Strategies have been developed to grow the graphene sheets with the area of up to 1 cm^2 using the chemical vapor deposition (CVD) of hydrocarbons (such as methane, CH_4) on copper, an abundant and inexpensive substrate [4–6]. Alongside the experimental efforts, modeling of the CVD graphene growth on Cu has also been attempted. These studies can be divided into three groups: *ab initio* and kinetic Monte Carlo (KMC) methods [7–9], rate equations [7,10], and phase-field methods [11]. By assuming the anisotropic diffusion on Cu of the carbon atoms and their anisotropic attachment to the islands, the authors of the latter reference succeeded in computing the growth of the multilobe graphene islands on the substrates of different crystallographic orientations. However, with the focus of the study on the morphologies, the kinetic maps of the growth-rate dependence on the controllable process parameters, such as the pressure and temperature, were not computed.

In this paper, we describe a simpler, one-dimensional partial-differential equation (PDE) model, whose purpose is to compute the growth rate of a single graphene island as a function of three control parameters: the crystallographic orientation of the substrate, the growth temperature, and the pressure of a gas of the carbon atoms that impinge on the substrate. In the manner of Ref. [11], we abstract from the details of the dissociation of a hydrocarbon, assuming that it results in the carbon gas from which the carbon atoms are adsorbed on the Cu surface. However, we recognize, as is pointed out in the *ab initio* studies, that besides the carbon atoms there are other diffusing species that may contribute to the island growth [3]—of which the carbon dimers are thought to be the most important [7,8,12]. Our hybrid model can be seen as an extension, directly informed by the activation energies from the *ab initio* calculations [7], of the classical BCF-type modeling [13] to two interacting and diffusing species that feed growth of the graphene island edge. This results in a coupled PDE problem for the concentration fields on the substrate. Both PDEs are also coupled, through the boundary conditions, to an ordinary-differential equation (ODE) for the position of the island edge.

II. MODEL FORMULATION

As we pointed out in Sec. I, the model is aimed at computing the velocity $\dot{x}_0(t)$ of a growing edge of a single-layer graphene island. Here, $x_0(t)$ is the position of the edge; see Fig. 1.

Since the edge grows predominantly by attachment of the carbon atoms and dimers [7,8,12], let $C(x,t)$ and $C_2(x,t)$ be the concentrations of the carbon atoms adsorbed on Cu and the carbon dimers, respectively. The latter result from the assembly of two previously adsorbed carbon atoms.

The model is comprised of the following PDEs and boundary conditions [14].

(i) Evolution equation for the concentration C on the section of the copper substrate that is not yet covered by the growing graphene island:

$$\frac{\partial C}{\partial t} = D_c \frac{\partial^2 C}{\partial x^2} - \chi_c C^2 + F, \quad -\ell \leqslant x \leqslant x_0(t). \tag{1}$$

Here, D_c is the carbon atoms diffusivity, F is the adsorption flux, and the sink term $-\chi_c C^2$ describes the loss of the carbon atoms due to their assembly into the dimers; the kinetics of this loss is reciprocal in t, e.g., $C \sim 1/\chi_c t$, as follows from the ODE $dC/dt = -\chi_c C^2$. We found that it is not necessary to include atom desorption in Eq. (1), particularly since the desorption rate has not been published and because even without the desorption the concentration is quite small (Fig. 2). Equation (1) is a well-posed nonlinear PDE with a unique solution for all $t > 0$ [15,16].

The boundary conditions for C are

$$x = -\ell : \frac{\partial C}{\partial x} = 0, \tag{2}$$

$$x = x_0(t) : -D_c \frac{\partial C}{\partial x} = K_c(C - C_{eq}). \tag{3}$$

The first boundary condition states that far from the graphene island (at the center of the substrate), the carbon concentration profile is symmetric. The second one states that at the growing edge, the flux of the carbon atoms is proportional to the difference between the concentration there and the equilibrium concentration [17]; the proportionality parameter K_c is the kinetic coefficient, which gives a measure of the ease with which the carbon atoms can attach to the edge.

(ii) Evolution equation for the concentration C_2, also on the section of the substrate not yet covered by the growing

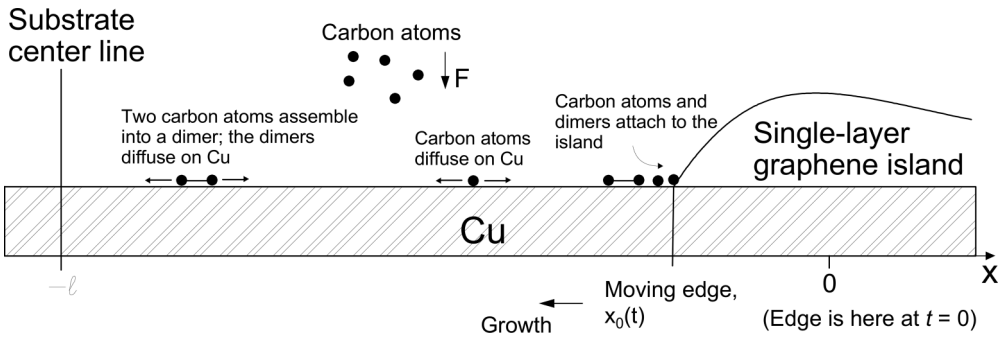

FIG. 1. Sketch of the graphene island growing on Cu, with the atomic events shown.

graphene island:

$$\frac{\partial C_2}{\partial t} = D_{c2}\frac{\partial^2 C_2}{\partial x^2} - \kappa_{c2}C_2 + \chi_c C^2, \quad -\ell \leqslant x \leqslant x_0(t). \tag{4}$$

Here, D_{c2} is the diffusivity of the carbon dimers, κ_{c2} is their desorption rate, and the source term $\chi_c C^2$ is due to assembly of the carbon atoms into dimers. Notice that through this term, the linear Eq. (4) is one-way coupled to Eq. (1).

The boundary conditions for C_2 mirror those for C,

$$x = -\ell : \frac{\partial C_2}{\partial x} = 0, \tag{5}$$

$$x = x_0(t) : -D_{c2}\frac{\partial C_2}{\partial x} = K_{c2}(C_2 - C_{eq2}). \tag{6}$$

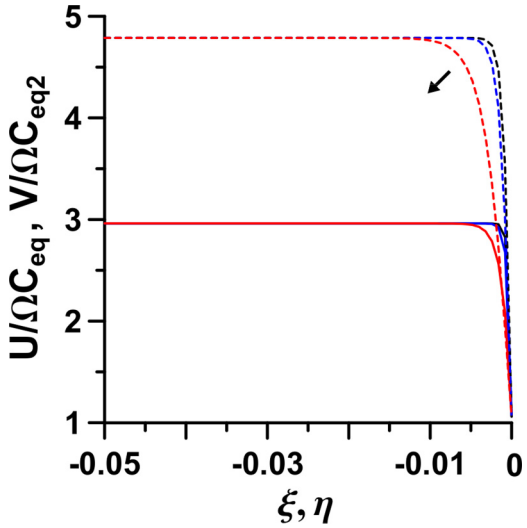

FIG. 2. Example dimensionless concentrations of the atoms (solid lines) and dimers (dashed lines), shown in units of the respective dimensionless equilibrium concentration, vs the transformed dimensionless coordinate along the Cu[111] substrate (see Sec. IV). $\xi = 0$ (or $\eta = 0$) corresponds to the growing edge. Time increases in the direction shown by the arrow (from the black to the red). Notice that the concentrations are not fixed at $\xi = 0$ [by the boundary conditions (19)]. Also notice that the dimers' concentration is larger than the one of the atoms, which corroborates the findings in the *ab initio* computations [7].

Here, K_{c2} is the attachment coefficient of the dimers and C_{eq2} is the equilibrium concentration for the growth by the dimers attachment.

(iii) Equation of the edge growth:

$$\dot{x}_0(t) = -\Omega K_c\{C[x_0(t),t] - C_{eq}\} - 2\Omega K_{c2}\{C_2[x_0(t),t] - C_{eq2}\},\ x_0(0) = 0. \tag{7}$$

This equation states that the edge velocity is the sum of the contributions resulting from the attachment of the atoms and dimers, where each contribution is proportional to the deviation at the edge of the corresponding concentration from its equilibrium value [17]. $\Omega = \pi a^2$ is the atomic area, where $a = 7 \times 10^{-9}$ cm is the radius of the carbon atom.

Equations (1)–(7) are made dimensionless by choosing ℓ, ℓ^2/D_c, and $1/\Omega$ as the length, time, and concentration scale, respectively. Keeping the same notations for the dimensionless variables, the dimensionless system reads

$$\frac{\partial C}{\partial t} = \frac{\partial^2 C}{\partial x^2} - \alpha C^2 + \beta, \tag{8}$$

$$\frac{\partial C_2}{\partial t} = D\frac{\partial^2 C_2}{\partial x^2} - \delta C_2 + \alpha C^2, \tag{9}$$

$$\dot{x}_0(t) = -R_c\{C[x_0(t),t] - \Omega C_{eq}\} - 2R_{c2}D\{C_2[x_0(t),t] - \Omega C_{eq2}\}, \quad x_0(0) = 0, \tag{10}$$

$$x = -1 : \frac{\partial C}{\partial x} = 0, \quad \frac{\partial C_2}{\partial x} = 0, \tag{11}$$

$$x = x_0(t) : \frac{\partial C}{\partial x} = R_c(\Omega C_{eq} - C), \quad \frac{\partial C_2}{\partial x} = R_{c2}(\Omega C_{eq2} - C_2). \tag{12}$$

Here the eight parameters are $\alpha = \chi_c\ell^2/D_c$ (the assembly rate of the atoms into the dimers), $\beta = F\Omega\ell^2/D_c$ (the adsorption flux of the atoms), $\delta = \kappa_{c2}\ell^2/D_c$ (the desorption rate of the dimers), $D = D_{c2}/D_c$ (the ratio of the diffusivities), $R_c = K_c\ell/D_c$ (the attachment rate of the atoms), $R_{c2} = K_{c2}\ell/D_{c2}$ (the attachment rate of the dimers), and ΩC_{eq} and ΩC_{eq2} (the dimensionless equilibrium concentrations).

The initial condition for C is taken in the form of a smoothed step function with a narrow transition, in the middle of the interval, from a smaller positive value at $x = -\ell$ to a larger

TABLE I. Activation energies (in eV).

Cu surface	E_{Dc}	E_{Dc2}	E_{χ}	E_{κ}	E_{Kc}	E_{Kc2}	E_{ad}	E_{Ceq}	E_{Ceq2}
[111]	0.5	0.49	0.9	1.7	0.71	0.74	0.1	0.87	0.87
[100]	1.11	0.62	0.59	1.7	1.42	1.07	0.1	0.87	0.87

value at $x = x_0(0) = 0$. Zero initial condition for C_2 is taken, e.g., at $t = 0$, there are no dimers on the substrate.

Apart from the multiple parameters, the system (8)–(12) looks deceptively simple. However, this is the moving-boundary problem, since the position $x_0(t)$ of the graphene edge is *a priori* unknown and must be found along with the concentrations. Due to a moving edge, any change in the concentrations' gradients near the edge affects the edge growth speed, and the change in speed in turn affects the concentrations near the edge and beyond. After focusing on the physical parameters in the next section, in Sec. IV the procedure for the numerical solution of this system of equations is described.

III. PHYSICAL PARAMETERS

All physical parameters are taken in the Arrhenius form, with the most recent and complete, to our knowledge, values of the activation energies [7] (see Table I). The preexponential factors are taken proportional to k_BT/h, where h is Planck's constant [10],

$$\begin{aligned} D_c &= \frac{k_BTa^2}{h}e^{-E_{Dc}/k_BT}, \quad D_{c2} = \frac{k_BTa^2}{h}e^{-E_{Dc2}/k_BT}, \\ \chi_c &= \frac{k_BT}{h}e^{-E_{\chi}/k_BT}, \quad F = \frac{P_0}{\sqrt{2\pi mk_BT}}e^{-E_{ad}/k_BT}, \\ \kappa_{c2} &= \frac{k_BT}{h}e^{-E_{\kappa}/k_BT}, \\ K_c &= \frac{k_BTa}{h}e^{-E_{Kc}/k_BT}, \quad K_{c2} = \frac{k_BTa}{h}e^{-E_{Kc2}/k_BT}, \\ C_{eq} &= \Omega^{-1}e^{-E_{Ceq}/k_BT}, \quad C_{eq2} = \Omega^{-1}e^{-E_{Ceq2}/k_BT}. \end{aligned} \tag{13}$$

Values for E_{κ}, E_{ad}, E_{Ceq}, and E_{Ceq2} were not published for graphene growth on copper. Thus, in Table I, we adopt the generic values for E_{ad}, E_{Ceq}, and E_{Ceq2} [18,19], and for E_{κ} we adopt a value that partially curtails the otherwise unlimited growth of the dimer concentration (caused by the perpetual assembly of the carbon atoms into dimers), allowing the computation to proceed until the edge grows over the entire available substrate. This value is large, and thus the desorption flux is small.

Carbon gas pressure P_0 is varied in the range 100–600 mTorr, $m = 2 \times 10^{-23}$ g is the molecular weight of carbon, the temperature T is in the interval 873–1273 K, and the half width of the substrate $\ell = 1$ mm.

IV. SOLUTION METHODS

Since solving PDEs on time-dependent domains is difficult, we first map the interval $-1 \leqslant x \leqslant x_0(t)$ onto a fixed interval $-1 \leqslant \xi \leqslant 0$ for the new space variable ξ, using the transformation

$$\begin{aligned} \xi &= \frac{x - x_0(t)}{1 + x_0(t)}, \quad C(x,t) = U(\xi(x,t),t), \\ C_2(x,t) &= V(\xi(x,t),t), \end{aligned} \tag{14}$$

where U and V are the concentrations of the atoms and dimers on the fixed interval. Then the system (8)–(12) takes the form

$$\begin{aligned} \frac{\partial U}{\partial t} &= \left[\frac{1}{1 + x_0(t)}\right]^2 \frac{\partial^2 U}{\partial \xi^2} + \dot{x}_0(t)\left[\frac{1+\xi}{1 + x_0(t)}\right]\frac{\partial U}{\partial \xi} \\ &\quad - \alpha U^2 + \beta, \end{aligned} \tag{15}$$

$$\begin{aligned} \frac{\partial V}{\partial t} &= D\left[\frac{1}{1 + x_0(t)}\right]^2 \frac{\partial^2 V}{\partial \xi^2} + \dot{x}_0(t)\left[\frac{1+\xi}{1 + x_0(t)}\right]\frac{\partial V}{\partial \xi} \\ &\quad - \delta V + \alpha U^2, \end{aligned} \tag{16}$$

$$\begin{aligned} \dot{x}_0(t) &= -R_c[U(0,t) - \Omega C_{eq}] \\ &\quad - 2R_{c2}D[V(0,t) - \Omega C_{eq2}], \; x_0(0) = 0, \end{aligned} \tag{17}$$

$$\xi = -1 : \frac{\partial U}{\partial \xi} = 0, \; \frac{\partial V}{\partial \xi} = 0, \tag{18}$$

$$\begin{aligned} \xi = 0 &: \frac{\partial U}{\partial \xi} = [1 + x_0(t)]R_c(\Omega C_{eq} - U), \\ \frac{\partial V}{\partial \xi} &= [1 + x_0(t)]R_{c2}(\Omega C_{eq2} - V). \end{aligned} \tag{19}$$

In the transformed system, the edge of the graphene island is at $\xi = 0$ at all times. However, the true edge position $x_0(t)$ is found from Eq. (17) and therefore the kinetics of growth is preserved. The system (15)–(19) is the initial-boundary value problem for two one-way coupled PDEs (with the variable coefficients), which are also coupled to the first-order ODE for $x_0(t)$. For the solution of this system, we adopted the classical method of lines (MOL), which converts the PDEs into ODEs by discretizing the space variable using finite differences. However, with the realistic physical parameters from Sec. III, the computed concentration profiles feature a steep boundary layer at the growing edge [see Fig. 2 and Figs. 8(a) and 8(b)]. For the prediction of the edge growth rate, it is crucial to resolve these layers with a high accuracy. We found that this is achieved by a method that we describe below.

First, the space variable ξ is transformed as [20]

$$\xi(\eta) = \eta + \frac{\gamma}{\pi}\sin \pi\eta, \quad -1 \leqslant \eta \leqslant 0, \quad |\gamma| < 1. \tag{20}$$

Notice that this map is invertible when the absolute value of the parameter γ is less than one; also, $\eta(0) = 0$, $\eta(-1) = -1$. The purpose of the transformation is to map the would-be nonuniform computational grid on $-1 \leqslant \xi \leqslant 0$ (where at $\gamma < 0$ the grid points are clustered near $\xi = 0$) onto a uniform grid on $-1 \leqslant \eta \leqslant 0$. In all computations, we used $\gamma = -0.95$.

Next, the final transformed system is discretized in η using the second-order finite differences with the fixed grid spacings h and $h/2$, and two ODE systems resulting from such discretizations are solved independently and in parallel using the same initial condition. Richardson interpolation is

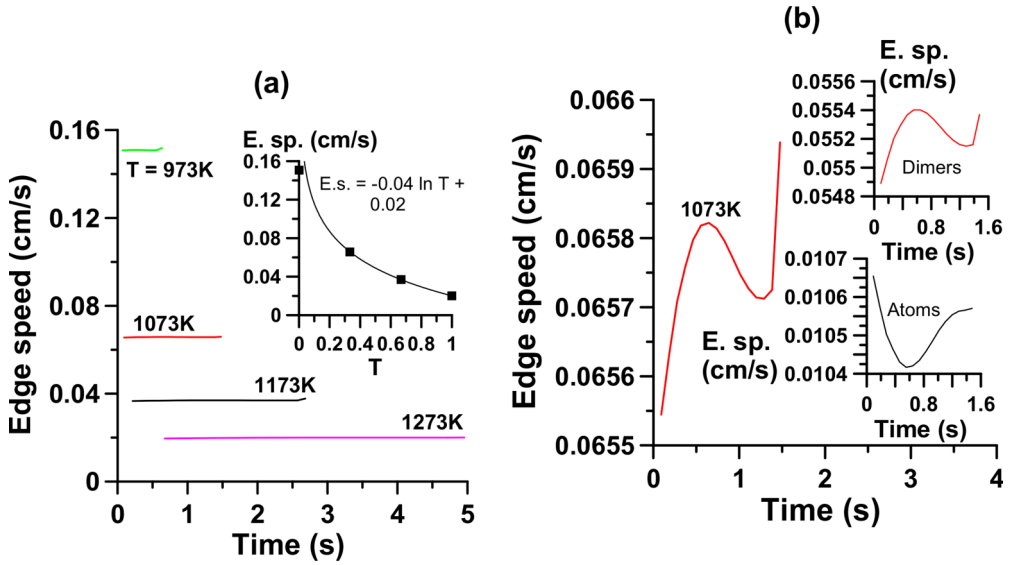

FIG. 3. Cu[111] surface. (a) Edge speed $|x_0(t)|$ vs the time at $P_0 = 500$ mTorr and various temperatures. The last point on each curve corresponds to the time t_{final} at which the edge reaches the midpoint of the substrate, $x = -\ell = -0.1$ cm. Inset shows the mean edge speed vs the temperature (that was first mapped onto the unit interval), where the mean is calculated over the time interval from zero to t_{final} for each curve; the line is the logarithmic fit to the data shown by squares. (b) Magnification of the $T = 1073$ K curve from (a). Insets show separately the components of this speed due to the attachment to the edge of the atoms and dimers.

performed after a fixed number of time steps. In this way, a spatially fourth-order accurate solution is obtained on a coarse grid. This solution is then interpolated onto a fine grid before the next step is taken. The temporal accuracy is achieved automatically by an ODE solver. The grid refinement study was performed, which indicated that using $h = 0.0008$ results in the needed overall computational accuracy for all parameters' values of interest.

V. RESULTS

We begin this section with the comparisons of Figs. 3 and 4, computed for graphene growth on a Cu[111] surface, with the corresponding Figs. 5 and 6 for the growth on a Cu[100] surface.

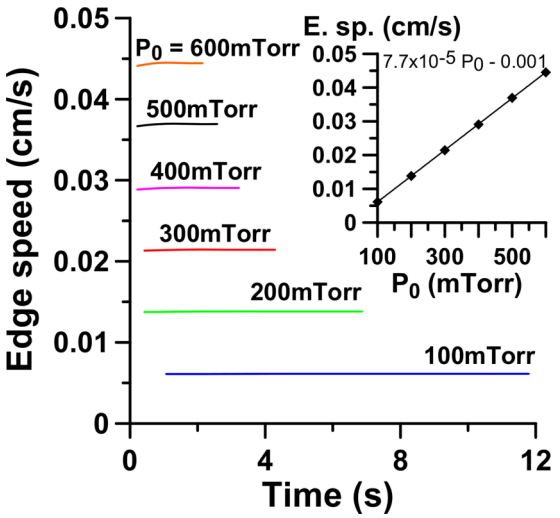

FIG. 4. Cu[111] surface. Edge speed vs the time at $T = 1173$ K and various pressures. Inset: the mean speed vs the pressure (squares) and the linear fit, also at $T = 1173$ K.

In Figs. 3(a) and 5(a), it can be seen that the growth slows down as the temperature increases, which perhaps explains the better graphene quality and larger islands at higher growth temperatures [1,4–6,12]. From the insets to these figures, it appears that the slowdown is logarithmic. This is an important model prediction, as the quantitative experimental results on the growth speed scaling with the temperature have not been published. At each temperature, the speed is nearly a constant value for the entire duration of the simulation [changing less than 1%; see Figs. 3(b) and 5(b)]. Also we noticed that the speed is smaller on Cu[100] and it slowly and monotonically decreases with time on this surface, while on a Cu[111] surface the curve is S-shaped; the latter dynamics is somewhat similar to the one shown in Fig. 2 of Ref. [4]. Attachment of the dimers provides the major contribution to the growth speed (see the insets). In the case of growth on Cu[111], the contribution from the dimers exceeds, by a factor of five, the one from the atoms; on Cu[100], the atoms provide a negligible contribution. This supports the recent conclusions in the *ab initio* [7,8] and experimental papers [4,5,12] that the graphene edge grows primarily by the dimer attachment.

Figures 4 and 6 show the dependencies of the edge speed on the time and pressure at a fixed temperature. The speed increases linearly with P_0. This is another key model prediction that remains to be supported by the experiment; the quantitative experimental data were not published. We remark here that the computed growth speeds shown in Figs. 3–6 exceed, by a few orders of magnitude, the speeds that are reported in the experimental papers. Values from the experiments seem to be of the order of 10^{-6}–10^{-5} cm/s for the temperature range that we use in the computations. We conjecture that the discrepancies are primarily due to the larger P_0 values used in our computations than the carbon partial pressures in

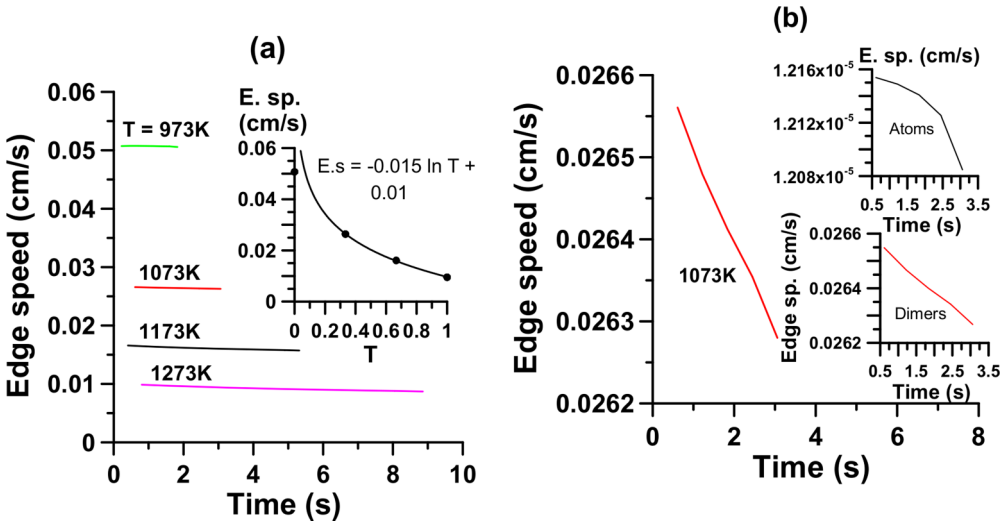

FIG. 5. Same as Fig. 3, but for a Cu[100] surface.

the experiments, as well as because the adopted E_{ad} value is approximate. Since the pressures of the hydrocarbons or the evaporated carbon are not consistently reported in the experimental literature, we took for P_0 the set of "growth pressure" (or "chamber pressure") values from Ref. [1]. From the inset of Fig. 4, one can see that the speed of the order 10^{-5} cm/s would result when the fit is extrapolated to $P_0 \sim 13$ mTorr (for the Cu[111] surface, see Fig. 6; this value is 21 mTorr). These extrapolated values are order-of-magnitude consistent with those reported in Refs. [4,12], in conjunction with the growth rates of the orders that we stated above.

It is common in the experiments to employ thermal cycles during growth or sharply decrease the temperature at the very end of the growth phase. This typically results in better quality of the graphene layer; also, its area is enlarged [5,21,22]. Why this happens is not well understood [23]. Our model is well suited for giving some insights into this situation. We started the computation using the parameters at 1273 K and computed for some time, then instantaneously switched to the parameters at 973 K and computed more, and finally switched back to the parameters at 1273 K and computed until the substrate overgrowth by a graphene sheet was completed. In Fig. 7, we show the growth speed, and in Fig. 8, the concentrations profiles. First, we notice that the growth speed is fully reversible, e.g., after the temperature is quenched from 973 to 1273 K, the speed returns to its value prior to the cool down. What is remarkable is the large factor (≈40) by which the speed increases (decreases) when the temperature is decreased (increased). This value can be directly compared to Fig. 3, which is computed at the same P_0 and at a *constant* temperature throughout the entire growth phase. There, the factor by which the speed changes is 7.5 when the temperature is dropped from 1273 to 973 K. Clearly, quenching the temperature down and then up during growth results in a large net increase of the growth speed (notice that the growth is completed in 1.6 s in Fig. 7 and in 5 s in Fig. 3). Closer examination shows that this increase is attributed nearly entirely to the dimers; their concentration experiences a much more abrupt change (compared to the concentration of the atoms) when the temperature is quenched up or down. This is

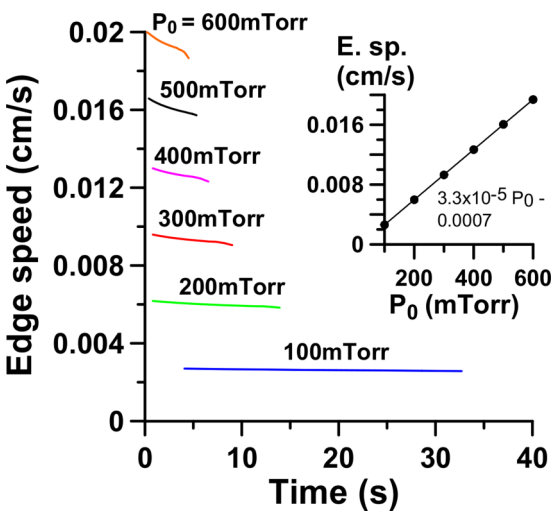

FIG. 6. Same as Fig. 4, but for a Cu[100] surface.

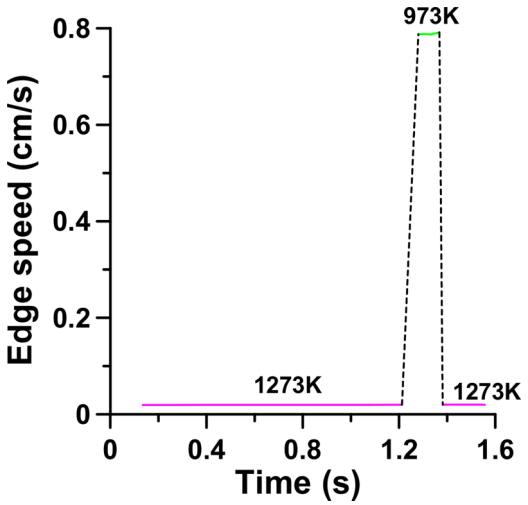

FIG. 7. Cu[111] surface, $P_0 = 500$ mTorr. The temperature is quenched from 1273 to 973 K and back.

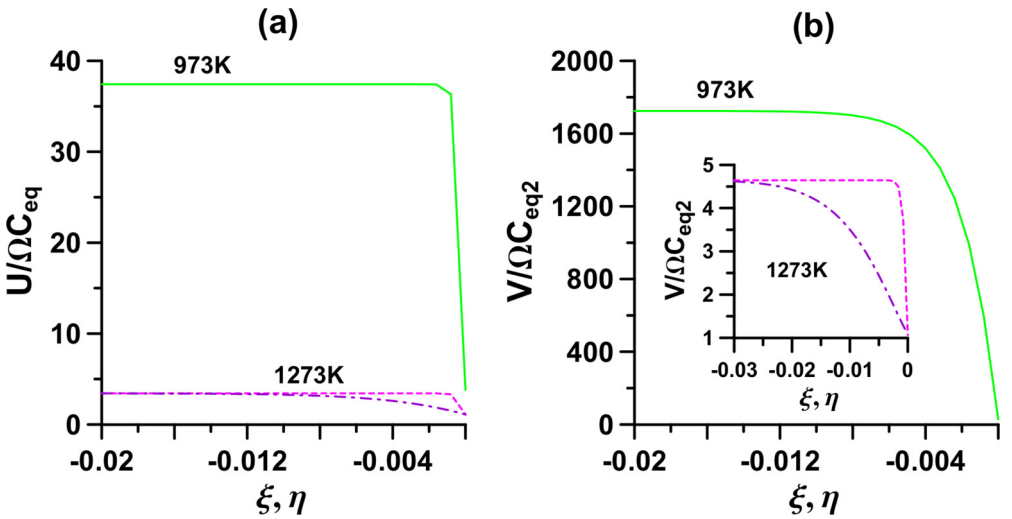

FIG. 8. Cu[111] surface, $P_0 = 500$ mTorr. (a) Atoms' concentrations at $T = 1273$ and 973 K before the cool down (dashed magenta line), after the cool down (solid green line), and after the warm up (dash-dotted purple line). (b) Dimers' concentrations; the line colors are the same as in (a).

shown in Fig. 8, where the concentrations are plotted before the cool down, after the cool down, and after the warm up. Such response of the concentrations to the temperature quenches is another indicator that the dimers are primarily responsible for the experimentally observed growth kinetics.

It was determined [4–6] that the growth slows down with time, increasingly so as the graphene islands more closely approach each other [6]. In the cited papers, the Cu crystallographic surface is not identified though; it is only stated that the growth is realized on a Cu foil. Also, since the observations are made when there are several growing islands, as is always the case, the growth slowdown might not occur were it possible to grow a single island. In our modeling, the minor decrease of the growth speed is seen for a Cu[100] surface, but not for a Cu[111] surface. However, it will be fairly straightforward to incorporate another growing island into the model, which may allow one to more precisely differentiate between the growth modes on these Cu surfaces. For better predictive capability, it may also be necessary to include the atoms' desorption term in Eq. (1) and the atoms' and dimers' deattachment rates (from the island) into Eq. (7), along with the corresponding source terms in Eqs. (1) and (4). It must be noted, though, that time-resolved graphene growth experiments that generate high-precision data on the growth rates, as well as the matching detailed descriptions of the plethora of the growth conditions and parameters, are still rare, which presents quite a challenge to further tuning the model.

ACKNOWLEDGMENTS

The author acknowledges constructive discussions with V. Dobrokhotov (WKU Applied Physics Institute).

[1] C. Mattevi, H. Kim, and M. Chhowalla, A review of chemical vapour deposition of graphene on copper, J. Mater. Chem. **21**, 3324 (2011).

[2] A. Reina and J. Kong, Graphene growth by CVD methods, in *Graphene Nanoelectronics: From Materials to Circuits*, edited by R. Murali (Springer Science and Business Media, New York, 2012), Chap. 7.

[3] H. Tetlow, J. Posthuma de Boer, I. J. Ford, D. D. Vvedensky, J. Coraux, and L. Kantorovich, Growth of epitaxial graphene: Theory and experiment, Phys. Rep. **542**, 195 (2014).

[4] X. Li, C. W. Magnuson, A. Venugopal, R. M. Tromp, J. B. Hannon, E. M. Vogel, L. Colombo, and R. S. Ruoff, Large-area graphene single crystals grown by low-pressure chemical vapor deposition of methane on copper, J. Am. Chem. Soc. **133**, 2816 (2011).

[5] Z. Yan, J. Lin, Z. Peng, Z. Sun, Y. Zhu, L. Li, C. Xiang, E. LoicSamuel, C. Kittrell, and J. M. Tour, Toward the synthesis of wafer-scale single-crystal graphene on copper foils, ACS Nano **6**, 9110 (2012).

[6] Z.-J. Wang, G. Weinberg, Q. Zhang, T. Lunkenbein, A. Klein-Hoffmann, M. Kurnatowska, M. Plodinec, Q. Li, L. Chi, R. Schloegl, and M.-G. Willinger, Direct observation of graphene growth and associated copper substrate dynamics by in situ scanning electron microscopy, ACS Nano **9**, 1506 (2015).

[7] P. Wu, Y. Zhang, P. Cui, Z. Li, J. Yang, and Z. Zhang, Carbon Dimers as the Dominant Feeding Species in Epitaxial Growth and Morphological Phase Transition of Graphene on Different Cu Substrates, Phys. Rev. Lett. **114**, 216102 (2015).

[8] P. Wu, W. Zhang, Z. Li, and J. Yang, Mechanisms of graphene growth on metal surfaces: Theoretical perspectives, Small **10**, 2136 (2014).

[9] P. Gaillard, T. Chanier, L. Henrard, P. Moskovkin, and S. Lucas, Multiscale simulations of the early stages of the growth of graphene on copper, Surf. Sci. **637–638**, 11 (2015).

[10] A. Zangwill and D. D. Vvedensky, Novel growth mechanism of epitaxial graphene on metals, Nano Lett. **11**, 2092 (2011).

[11] E. Meca, J. Lowengrub, H. Kim, C. Mattevi, and V. B. Shenoy, Epitaxial graphene growth and shape dynamics on copper: Phase-field modeling and experiments, Nano Lett. **13**, 5692 (2013).

[12] K. Celebi, M. T. Cole, J. W. Choi, F. Wyczisk, P. Legagneux, N. Rupesinghe, J. Robertson, K. B. K. Teo, and H. G. Park, Evolutionary kinetics of graphene formation on copper, Nano Lett. **13**, 967 (2013).

[13] W. K. Burton, N. Cabrera, and F. C. Frank, The growth of crystals and the equilibrium structure of their surfaces, Phil. Trans. R. Soc. A **243**, 299 (1951).

[14] See A. L.-S. Chua, E. Pelucchi, A. Rudra, B. Dwir, E. Kapon, A. Zangwill, and D. D. Vvedensky, Theory and experiment of step bunching on misoriented GaAs(001) during metalorganic vapor-phase epitaxy, Appl. Phys. Lett. **92**, 013117 (2008) for a somewhat similar PDE model of the multispecies crystal growth (not specialized for particularities of the graphene growth).

[15] H. A. Levine, The role of critical exponents in blowup theorems, SIAM Rev. **32**, 262 (1990).

[16] K. Vijayakumar, On the integrability and exact solutions of the nonlinear diffusion equation with a nonlinear source, J. Austral. Math. Soc. Ser. B **39**, 513 (1998).

[17] M. Uwaha, Fluctuation and morphological instability of steps in a surface diffusion field, in *Advances in the Understanding of Crystal Growth Mechanisms*, edited by T. Nishinaga *et al.*, (Elsevier, New York, 1999), pp. 31–45.

[18] W. Hong, Z. Suo, and Z. Zhang, Dynamics of terraces on a silicon surface due to the combined action of strain and electric current, J. Mech. Phys. Solids **6**, 267 (2008).

[19] G. Schulze Icking-Konert, M. Giesen, and H. Ibach, Decay of Cu adatom islands on Cu (111), Surf. Sci. **398**, 37 (1998).

[20] W. F. Spotz and C. F. Carey, Formulation and experiments with high-order compact schemes for nonuniform grids, Intl. J. Num. Methods Heat Fluid Flow **8**, 288 (1998).

[21] L. Gao, J. R. Guest, and N. P. Guisinger, Epitaxial graphene on Cu(111), Nano Lett. **10**, 3512 (2010).

[22] A. A. Koos, A. T. Murdock, P. Nemes-Incze, R. J. Nicholls, A. J. Pollard, S. J. Spencer, A. G. Shard, D. Roy, L. P. Biro, and N. Grobert, Effects of temperature and ammonia flow rate on the chemical vapour deposition growth of nitrogen-doped graphene, Phys. Chem. Chem. Phys. **16**, 19446 (2014).

[23] H. Kim, E. Saiz, M. Chhowalla, and C. Mattevi, Modeling of the self-limited growth in catalytic chemical vapor deposition of graphene, New J. Phys. **15**, 053012 (2013).